

Photon emission in heavy ion collisions at the CERN SPS

P. Huovinen^{a,b,1} P.V. Ruuskanen^{c,2} S.S. Räsänen^{c,2}

^a*Lawrence Berkeley National Laboratory, Berkeley, CA 94720, USA*

^b*School of Physics and Astronomy, University of Minnesota,
Minneapolis, MN 55455, USA*

^c*Department of Physics, University of Jyväskylä, P.O.Box 35, FIN-40351 Jyväskylä,
Finland*

Abstract

We compute the thermal photon spectrum in the Pb+Pb collisions at the CERN SPS energy using thermal emission rates and a hydrodynamic description for the evolution of produced hot matter and compare our results with the measurements of the excess photons by the WA98 collaboration. Our results show that the measured photon spectrum can be reproduced with realistic initial conditions which take properly into account also the finite longitudinal size of the initial collision zone and which simultaneously describe well both the transverse and longitudinal hadron spectra. In the scenario with initial formation of QGP the recently calculated emission rate, complete to order α_s , reproduces the measured spectrum. However, the experimental spectrum can also be reproduced in a purely hadronic scenario without transition to QGP state, but a high initial temperature, much over the values predicted for the phase transition temperature T_c , is required.

¹huovinen@physics.umn.edu

²vesa.ruuskanen, sami.rasanen@phys.jyu.fi

1 Introduction

For the study of the properties of matter created in a high energy heavy-ion collision, photons and lepton pairs provide the most direct probe since, after being emitted, they escape the system without further interactions. Unfortunately, electromagnetic interactions occur during all the different stages of the collision, ranging from those between the incoming partons to the decays of final hadrons, and it is difficult to disentangle experimentally the contributions from these different sources.

After a painstaking analysis, the WA98 collaboration has succeeded in isolating an excess of photons over those originating from the decays of final hadrons [1, 2]. Since a QCD calculation of photon production from the primary interactions of incoming partons fails to reproduce this excess¹ [2, 3], they can be associated with the secondary interactions of final state particles. In a phenomenological analysis of heavy-ion collisions, based on the assumption of the formation of a thermal system, these are often called the thermal photons.

Since the publication of the WA98 data there has been several attempts to describe the data using a thermal description for the expanding matter [5, 6, 7, 8, 9] and the calculated thermal emission rates of photons. In these studies the time evolution of matter has either been given by a simple parameterization of spherical expansion [9] or described by using boost invariant hydrodynamics [5, 6, 7, 8]. In the papers applying hydrodynamics, the reproduction of the data has required either large initial temperature which led to unrealistically short initial time for boost invariant flow [5], significant initial radial velocity [6, 7, 8], or large modifications in hadron masses [6].

In the papers applying hydrodynamics [5, 6, 7, 8] the validity of boost invariant expansion is taken at face value. However, from the hadron data at the SPS, we know that the rapidity window where the expansion is boost invariant is narrow if it exists at all. Even if the flow is approximately boost invariant at later times, it can be expected to deviate from the scaling behaviour for $\tau \lesssim 1$ fm/c because of the finite longitudinal extent of the collision zone as discussed in more detail below. It is also known [10] that if the assumption of boost invariance is relaxed and the longitudinal expansion is constrained to reproduce the measured rapidity spectra of hadrons, the initial energy densities become strongly peaked and larger by a factor two than the Bjorken estimate. As is evident in [5] the thermal photon production at large k_T is very sensitive to initial temperature and dominated by the earliest moments of the expansion. Therefore, the photon production even at midrapidity becomes sensitive to the details of the initial state including its longitudinal structure.

In this letter we take a conservative approach to photon production. We use well known vacuum properties of mesons also in dense medium and set the initial radial velocity to zero. Instead of studying these effects we concentrate on the effects on photon

¹ It should be kept in mind that a consistent description of inclusive photon data in hadronic collisions in fixed target experiments is difficult to achieve [4].

spectra caused by different initial states and equations of state (EoS) of the expanding matter. In all cases the calculation is constrained to provide a reasonable description of both transverse and longitudinal hadronic spectra [11], not only the final particle multiplicity as in [5, 6, 8]. In our model finite baryon number density is included in the EoS. We assume local chemical equilibrium with zero strangeness density until kinetic freeze-out. This allows a reasonable reproduction of charged particle and net proton spectra but fails to describe the details of strange particle yields. However, this is not a severe problem since reproduction of negative particle spectra means the description of the bulk of the matter is realistic. The processes involving strange particles are not included in the photon production rates in hadron gas either. To compare with the results in literature, we calculate the photon spectra also with boost invariant expansion. As thermal production rates we use rates provided in the literature. For the QGP we use the recently obtained full order of α_s result [12, 13] for zero quark chemical potential, $\mu_q = 0$. This result contains both the lowest order one-loop rates [14, 15] with exact non-logarithmic term and completes the earlier two-loop calculations [16, 17] through summation of leading contributions from multi-loop terms up to all orders. In hadron gas we use the parameterizations [18, 19] of the rates calculated using effective Lagrangians and vector-dominance model [14, 19].

2 The framework for calculating thermal spectra

Consider first the emission rates of photons from a thermal matter. Since we assume that the photons escape the system after emission the emitted spectrum is not the thermal, black-body radiation spectrum.

In the QGP one is faced with the problem of infrared singularities in the rate calculation. In lowest order this leads to a logarithmic energy dependence on ω/T in addition to the usual exponential (in Boltzmann approximation) $\exp\{-\omega/T\}$ dependence [14, 15]. The next-to-leading order 2-loop result [16, 17] turned out to be of the same order in α_s and of the same size or larger than the leading 1-loop result. It was argued that also the leading parts of the higher-loop contributions are of order α_s [20]. Recently the resummation of order α_s contributions from all orders in the multi-loop expansion was achieved, fully completing the order of α_s analysis of the photon emission rate in the quark-gluon plasma [12, 13]. In our calculation we use the parameterization of the rate provided in [13]. It should be remembered that this result is for zero baryochemical potential whereas in the collisions at SPS energy net baryon density is relatively high. In the leading order, the effect of non-zero μ_q has been considered [21] and, in good approximation, it was found to be included into the rate by replacing the multiplicative factor T^2 by $T^2 + \mu_q^2/\pi^2$. We have checked that in the plasma phase the ratio of these factors is typically $1.02 < 1 + \mu_q^2/(\pi T)^2 < 1.05$ indicating only a few per cent increase to the calculated plasma contributions.

Another problem in applying the calculated rates in nuclear collisions is that the assumption of high temperature limit with an ideal QGP may not be valid. The lattice QCD calculations of energy density and pressure indicate that the ideal gas or Stefan–Boltzmann limit is approached slowly with increasing temperature [22]. On the other hand recent lattice calculations on lepton pair emission rate [23] show that, at least in some parts of the phase space, the lowest order (in α_s) perturbative result is quite close to the full lattice result. This is encouraging for the type of phenomenological study as presented here and supports the interpretation of data in terms of results based on perturbative rates.

In the hadron gas the scattering processes $\pi\pi \rightarrow \rho\gamma$ and $\pi\rho \rightarrow \pi\gamma$ are included in the photon emission rate. In addition to the contributions from interactions described with a pseudoscalar-vector Lagrangian [14], the process $\pi\rho \rightarrow \pi\gamma$ gets a large contribution from the $\pi\rho$ interaction with the a_1 axial meson: $\pi\rho \rightarrow a_1 \rightarrow \pi\gamma$ [19]. In our calculations we use the parameterizations provided by the authors in [18, 19] for these rates. Since in the WA98 analysis the decay contributions of final state hadrons are subtracted, only those $\rho \rightarrow \pi + \pi + \gamma$ and $\omega \rightarrow \pi^0 + \gamma$ decays which occur in the hadron gas before freeze-out are included. Even though the decays of final π^0 's and η 's dominate the decay photons from final hadrons, their decays are so much slower than those of ρ and ω that they can be neglected during the hadron gas phase. The effects of baryons on the emission rates are not known and our results contain rates from mesonic processes only. In the hydrodynamic calculation of expansion baryons are included.

We study the evolution of the system using three different equations of state (EoS). Two of the EoSs describe a first order phase transition from hadron gas to QGP with transition temperatures 165 MeV (EoS A) and 200 MeV (EoS D) and the third one describes the matter as a hadron gas also at high temperatures (EoS H). The QGP is an ideal gas of quarks with 2.5 flavours and gluons. The hadron gas contains all known hadrons with masses up to 2 GeV. A more detailed discussion can be found in [11, 24]. The present results from lattice calculations for the transition temperature are $T_c(n_f = 3) = 154 \pm 8$, $T_c(n_f = 2) = 173 \pm 8$, and $T_c(n_f = 2) = 171 \pm 4$ MeV, where the first two values are for improved staggered fermions and the last one for Wilson fermions [22]. For this reason we consider the EoS A with $T_c = 165$ MeV as our reference EoS.

As described in the introduction we want to study the effects of initial conditions on the longitudinal expansion and the photon production. For that purpose we do the calculation using three different descriptions of initial state. For two of them, labeled IS 1 and IS 2, the longitudinal expansion is not boost invariant. To be able to distinguish what is the effect of longitudinal expansion, we also carry out the calculations using the boost invariant expansion scenario (labeled BI in the following). When the expansion is not boost invariant, we assume that the rapidity distribution of energy in the initial state is Gaussian. The width of the rapidity distribution increases with the

	IS 1		IS 2		BI (0.3)	BI (1.0)
	EoS A	EoS H	EoS A	EoS H	EoS A	EoS A
T_{\max} (MeV)	325	275	265	245	364	244
$\bar{T}(z=0)$ (MeV)	255	234	214	213	301	214

Table 1: Maximum value and average initial temperature for different EoS and initial state. Average temperature is calculated at $z = 0$.

transverse coordinate r since the nuclei become more transparent towards the edges. The normalization is fixed by requiring the energy per unit transverse area in the initial state, $e(t_0, r) = \int dz T^{00}(t_0, r, z)$, to equal the energy per unit transverse area of incoming nucleons [10].

To convert this distribution to spatial energy density distribution we have to specify the z dependence of the initial longitudinal velocity. This choice is by no means unambiguous and since the choice of the velocity profile affects the maximum initial temperature and thus the photon yield, we carry out the calculations using two different profiles. In both cases the longitudinal size of the system is constrained to 3.2 fm and the longitudinal flow velocity at the edge of the system is similar. In the case of IS 1 we assume that the longitudinal flow rapidity increases linearly with distance z from the center of the system. In our second choice IS 2 the dependence is nonlinear and the velocity is smaller at small z , but becomes at large z larger than in the linear case IS 1 (see ref. [11]). In the case of IS 1 the energy density is strongly peaked in the middle whereas IS 2 leads to an almost flat distribution. Consequently IS 1 leads to a larger value of the maximum initial temperature than IS 2 (see table 1). In the following we use IS 1 as our reference expansion scenario.

In the case of boost invariant longitudinal flow, $v_z = z/t$, we assume the transverse distribution of energy density $\epsilon(\tau_0, r)$ to be proportional to the number of participants per unit transverse area. Its normalization is chosen to reproduce the observed pion p_T distribution in most central collisions [25]. The normalization of ϵ obviously depends on the initial time τ_0 which is the time for all the matter in the given rapidity range to reach local thermal equilibrium. In the boost invariant scenario this represents the main uncertainty of the calculation. It should be observed that the hadron spectra are not very sensitive to τ_0 as long as τ_0 is much shorter than the transverse time scale $\sqrt{3}R_A$ and if the initial densities are chosen to give the same total entropy. However, since the photon rates have a strong temperature dependence, especially the high- k_T part of the thermal photon spectrum changes considerably with different choices of τ_0 . To illustrate this effect, we carry out the boost invariant calculation for two different initial times, $\tau_0 = 1.0$ and 0.3 fm/c, labeled BI (1.0) and BI (0.3), respectively. In both

cases we fix the initial densities by taking the density profile used in [25] at $\tau_0 = 0.8$ fm/c and scale it to initial times $\tau_0 = 0.3$ and 1.0 fm/c by requiring that entropy per unit rapidity does not change.

At finite collision energy the longitudinal size of the collision zone is $\sim 2R_A/\gamma_{\text{cm}}$ which is also the measure of the time interval for the primary particle production. Since in the boost invariant expansion the longitudinal size of the system is $\sim 2\tau$, the initial time should satisfy $\tau_0 \gtrsim R_A/c\gamma_{\text{cm}} \sim 1$ fm/c for a consistent use of scaling hydrodynamics at SPS.² Even though we do not consider initial times as short as $\tau = 0.3$ fm to be realistic for a boost invariant expansion at the SPS, they may be useful in estimating the limits of photon spectra. In scenarios without boost invariance, the essential initial parameter is the longitudinal size of the system. In fixing the longitudinal size from the longitudinal collision geometry we have implicitly assumed that local thermalization times are shorter than this longitudinal scale.

3 Results

We have calculated the photon emission for all the combinations of three equations of state, EoS A, D and H, and the initial conditions, IS 1 and IS 2. For comparison we have performed the calculation also for the initial conditions BI(0.3) and BI(1.0) with EoS A. To illustrate the quality of our hydrodynamic description of the nuclear collision, we show in fig. 1 the measured π^0 spectrum with our calculated results for some of the cases we have studied. The solid line (IS 1, EoS H) and the dashed line (IS 2, EoS A) are the two extreme cases for the calculations with the non-scaling longitudinal expansion. All other combinations of non-scaling flow and EoS give spectra within these limits. The dotted (BI(0.3), EoS A) and dashed-dotted (BI(1.0), EoS A) lines represent calculations with boost invariant longitudinal flow, EoS A and initial conditions from [25] scaled to $\tau_0 = 0.3$ and 1.0 fm, respectively. We have not tried to fit the π^0 spectrum but, instead, used the same initial conditions as in earlier studies of hadron spectra from several SPS lead-lead experiments [11, 25].

In fig. 2 we show the contribution from the hadron gas (dotted line) and contributions from plasma using the 1-loop rate (dashed-dotted line), the sum of 1-loop and the order of α_s part of 2-loop rates (dashed line) and the total order of α_s rate obtained summing the contributions from multi-loop calculations up to all orders. The initial conditions IS 1 is used in the calculation. We conclude that the emission from plasma is dominant for the large transverse momentum range, $k_T > 2$ GeV. The suppression of the 2-loop result due to the resummation of higher loop contributions is roughly 30 % and the

²In [26] a saturation criterion for minijet production is presented leading to a time scale ~ 0.3 fm/c at the SPS. This is the time scale for the production of a minijet of transverse momentum ~ 0.7 GeV and, at the SPS, cannot be taken as the time interval for the formation of all minijets. Indeed, it is not clear if the saturation applies or if soft processes with a longer time scale are more significant at the SPS.

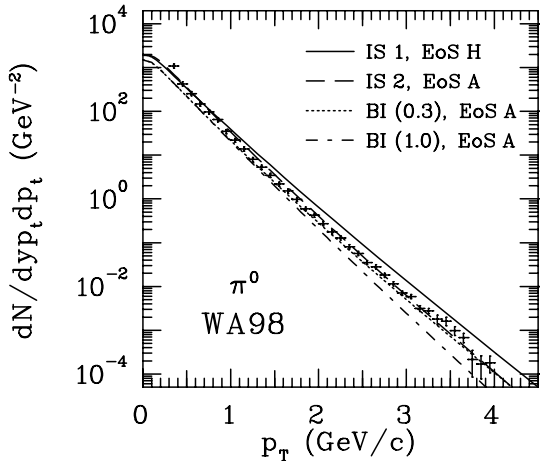


Figure 1: Calculated π^0 p_t -distribution for different initial states and EoSs compared with the measurement by the WA98 collaboration [1]. For details, see the text.

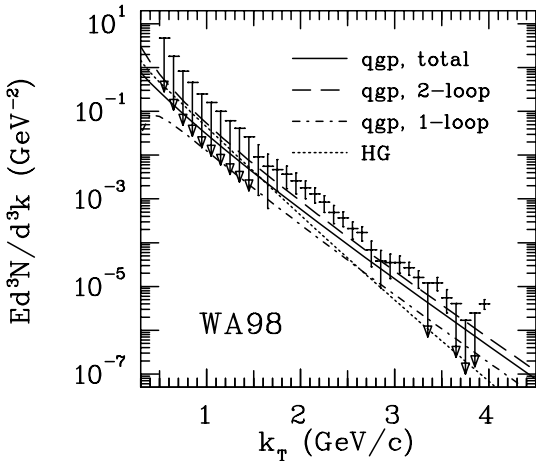


Figure 2: Thermal photon emission (IS 1 and EoS A) compared with the WA98 data [1]. The contribution from plasma is shown for rates calculated in leading order (1-loop), next to leading order (2-loop) and in order α_s with contributions from multi-loop calculations in all orders (total). Photons from hadronic phase are shown separately (HG).

1-loop contribution is typically $\sim 40\%$ of the total QGP rate. The shapes of the three plasma curves are remarkably similar.

In fig. 3 the total photon spectra are depicted for different initial conditions using EoS A in each case. As discussed in chapter 2, the initial values of energy density or equivalently of temperature are smaller for initial conditions IS 2 than for IS 1. In case of IS 2 the photon emission is reduced as compared to IS 1, especially at larger values of k_T . At later times the evolution is quite similar in both cases and the contributions from hadron gas do not differ significantly. For IS 2 the high- k_T end of the spectrum is not reproduced.

We show in fig. 3 also the results from calculations with longitudinal boost invariance starting the evolution either at $\tau_0 = 1$ or 0.3 fm/c with the same entropy per unit rapidity, dS/dy , in both cases. With this choice of initial times the results follow closely the nonscaling calculations so that for $\tau_0 = 0.3$ fm/c (BI(0.3)) the spectrum is close to that from initial conditions IS 1 and for $\tau_0 = 1$ fm/c (BI(1.0)) to that from IS 2. The high- k_T data is reproduced only with high temperature initial states, BI(0.3) for the longitudinal scaling flow and IS 1 for the non-scaling case. Since the cooling due to the longitudinal scaling expansion is very fast in the case of short initial time, a much

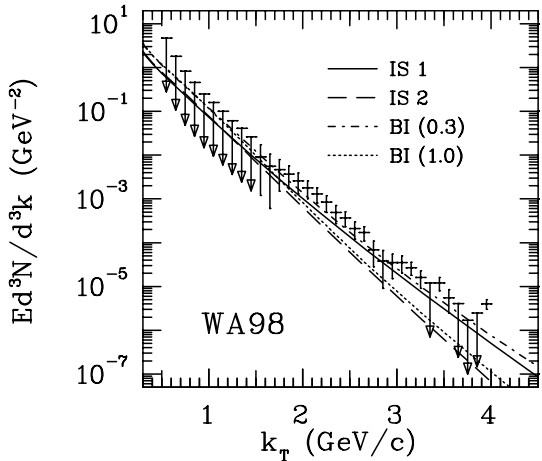


Figure 3: Thermal photon emission for different initial states. Data are from [1] and calculations are done using EoS A and total order of α_s rates in the plasma.

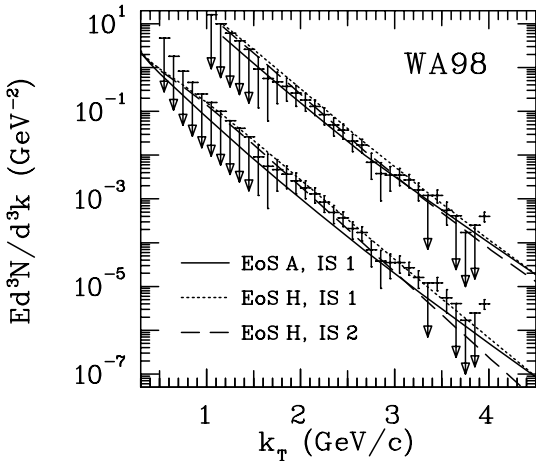


Figure 4: Thermal photon emission for different EoS and initial state with the contribution of initial pQCD photons (upper set) and without (lower set). The data and results of the upper set have been scaled by a factor 100.

higher initial temperature is needed in case of BI (0.3) than in case of IS 1, see table 1.

As was argued in the previous chapter, we do not consider the use of a short initial time, such as $\tau_0 = 0.3$ fm/c, to provide a fully consistent description of the early stage of a heavy-ion collision at the SPS energy even though the flow at mid rapidities at later times might evolve close to scaling flow. We have seen, however, that the early hot stage is essential for photon emission emphasizing the need for its reliable description. One could argue that the longitudinal size of the collision region is reduced below ~ 2 fm by shock compression but this would also slow down the initial flow from the scaling velocity $v_z = z/t$. In fact, this would lead to an initial state with even higher temperatures and slower expansion velocity than the one described by IS 1 and consequently to results overshooting the measured photon spectrum.

Part of the measured prompt photon spectrum is expected to come from the primary parton–parton interactions of incoming nuclei. A perturbative QCD analysis, which includes also a study of the effect of intrinsic transverse momentum of partons, gives results which are not more than 30 % of the measured spectrum when $\langle p_T^2 \rangle_{\text{intr}} = 0.9$ GeV 2 [3]. If no intrinsic partonic p_T is included, calculations are an order of magnitude below the data. A comprehensive analysis of prompt photons in hadron-hadron collisions at comparable energies does not favour large values of intrinsic $\langle p_T^2 \rangle$ [4]. It looks unlikely that the WA98 photon data can be explained in terms of pQCD photons from interactions of incoming partons but it would be premature to claim that this

possibility is definitely excluded.

In fig. 4 we show the photon spectra for EoS A using initial conditions IS 1 and for EoS H using both initial conditions IS 1 and IS 2. We have performed the calculations also for the EoS D with $T_c = 200$ MeV. Even though the different contributions change, the total spectra are qualitatively similar for EoS A and EoS D³. The reason to this is that at high k_T the highest temperatures dominate and they are not changed. The higher production rate of photons in hadron gas than in plasma [17] leads to a higher yield for EoS H and IS 1 than for EoS A and IS 1 even though the initial temperature is higher in the latter case (cf. table 1). The spectrum reaches the upper limits of experimental data points around $k_T \sim 2$ GeV when EoS H and IS 1 are used. The choice of initially cooler initial state IS 2 with EoS H decreases the yield sufficiently in $k_T \sim 2$ GeV region but also creates a distinctive convex shape of the spectrum.

To get a better understanding of the total photon yield in different cases we have parameterized the pQCD photon spectrum of [3] as presented in [27] and added it to the thermal yield. Resulting spectra are displayed as the upper set of curves in fig. 4 for $k_T > 1.2$ GeV. The differences are small both in normalization and shape. We feel that with the present accuracy of the data a χ^2 fitting would not be useful in ruling out any of the curves. The hadronic alternative, EoS H, with high temperature initial state IS 1 tends to stay above the data. The hadronic EoS with the lower density initial state, IS 2, goes through the data but there is a tendency for the curve to be slightly steeper than the data. The spectrum obtained by assuming a phase transition, EoS A and initial state IS 1 gives a very good description of data and seems, in particular in the shape, to be closest to the data.

We should like to point out that even with the initial state IS 2 the maximum value of the initial temperature in the hadron gas alternative is 245 MeV (cf. table 1). We have checked that for the high- k_T region, contributions from the short time interval with highest temperatures dominate. In all scenarios the contribution from matter with temperature $T < 200$ MeV is roughly 40 % of the total thermal yield at $k_T \simeq 3$ GeV.

4 Discussion and conclusions

We have studied in detail the dependence of thermal photon emission in central lead-lead collisions at CERN SPS describing hydrodynamically the expansion of produced matter and using known emission rates in hot matter. We have considered emission both from QGP and hadron gas and compared with each other the different contributions to the thermal rate. In the hydrodynamic calculations we have used hadronic spectra to constrain the initial conditions including the longitudinal structure. The significance of initial conditions is emphasized by the fact that most of the photons, in

³In ref. [11] the difference between the yields for EoS A and D was larger than here because we used only lowest order production rates.

particular at high k_T , are emitted in a short time interval right in the beginning of the expansion. For comparison we performed also the boost invariant calculation.

We find that the measured photons can be described in terms of a thermal model with hydrodynamical expansion either by using EoS A with phase transition or EoS H with hadron gas phase only. The model is constrained to reproduce the transverse and longitudinal hadron spectra. However, in describing the photon emission a high temperature initial state must be assumed. With the longitudinal scaling expansion this is achieved by choosing a short initial time $\tau_0 = 0.3$ fm/c which is not in complete accordance with longitudinal geometry. The need for high temperature initial state can be avoided by assuming a non-zero initial transverse velocity in case BI(1.0). We have tried this but, e.g. the use of a linearly increasing initial velocity as in ref. [7] with $v_r(r = R_A) = 0.3$, which produces very closely the same photon spectrum as IS 1 or BI(0.3) in fig. 3, leads to a π^0 spectrum well above the case IS 1, EoS H in fig. 1. We cannot lower the π^0 spectrum by simply decreasing the initial temperature since we would then go below the hadron multiplicities.

The shape of the photon spectrum clearly depends on whether phase transition is assumed or not. Unfortunately this dependence can not be used yet to differentiate between scenarios since the differences become as small or smaller than the experimental errors when the initial pQCD photons are added to the spectrum. One may argue that after the addition of initial pQCD contribution the spectrum with EoS A and IS 1 still reproduces the shape best, but the differences are small.

With QGP formation we find the higher-loop contributions essential for reproducing the data over the whole observed range. In particular, the shape of the spectrum follows the shape of the data and the normalization leaves room for the initial pQCD photons which are estimated to be of order 1/3 of the data with spectral shape very similar to that of the data. On the other hand, the experimental data rules out, within the thermal model, an increase of the rate by a large factor. This could be interpreted as lending support for the assumption that the emission rate of photons from plasma can be calculated perturbatively already in the temperature range 200 . . . 250 MeV and the main part of the rate is given by the full order of α_s result [12, 13].

In summary, the WA98 photon data supports a realistic thermal model with high density and temperature initial state constructed to describe the main features of hadron data. The spectra obtained by assuming a phase transition, EoS A, or pure hadron gas, EoS H, deviate somewhat in properties but the accuracy of the present data and the present understanding of initial pQCD photons is not enough to rule out either alternative.

Acknowledgements: We are grateful to P. Arnold, G. D. Moore and L. G. Yaffe for sending us a parameterization of their rates, P. Aurenche, F. Gelis and H. Zaraket for explaining theirs and M. Thoma for discussions and comments. This work was partly

supported by the U.S. Department of Energy under Contract No. DE-AC03-76SF00098 and Grant No. DE-FG02-87ER40328 and by the Research Council for Natural Sciences and Engineering of the Academy of Finland. P.H. thanks the University of Jyväskylä for hospitality while writing this paper.

References

- [1] M. M. Aggarwal *et al.* [WA98 Collaboration], Phys. Rev. Lett. **85** (2000) 3595 [nucl-ex/0006008].
- [2] M. M. Aggarwal *et al.* [WA98 Collaboration], nucl-ex/0006007.
- [3] C. Wong and H. Wang, Phys. Rev. C **58** (1998) 376 [hep-ph/9802378].
- [4] P. Aurenche M. Fontannaz, J.Ph. Guillet, B. Kniehl, E. Pilon, M. Werlen, Eur. Phys. J. C **9** (1999) 107.
- [5] D. K. Srivastava and B. Sinha, Phys. Rev. C **64** (2001) 034902 [nucl-th/0006018].
- [6] J. Alam, S. Sarkar, T. Hatsuda, T. K. Nayak and B. Sinha, Phys. Rev. C **63** (2001) 021901 [hep-ph/0008074]; J. Alam, P. Roy, S. Sarkar and B. Sinha, nucl-th/0106038.
- [7] D. Y. Peressounko and Y. E. Pokrovsky, hep-ph/0009025.
- [8] A. K. Chaudhuri, nucl-th/0012058.
- [9] K. Gallmeister, B. Kampfer and O. P. Pavlenko, Phys. Rev. C **62** (2000) 057901 [hep-ph/0006134].
- [10] J. Sollfrank, P. Huovinen and P. V. Ruuskanen, Eur. Phys. J. C **6** (1999) 525 [nucl-th/9801023].
- [11] P. Huovinen, P. V. Ruuskanen and J. Sollfrank, Nucl. Phys. A **650** (1999) 227 [nucl-th/9807076].
- [12] P. Arnold, G. D. Moore and L. G. Yaffe, JHEP **0111** (2001) 057 [hep-ph/0109064].
- [13] P. Arnold, G. D. Moore and L. G. Yaffe, JHEP **0112** (2001) 009 [hep-ph/0111107].
- [14] J. Kapusta, P. Lichard and D. Seibert, Phys. Rev. D **44** (1991) 2774 [Erratum-ibid. D **47** (1991) 4171].
- [15] R. Baier, H. Nakkagawa, A. Niegawa and K. Redlich, Z. Phys. C **53** (1992) 433.
- [16] P. Aurenche, F. Gelis, R. Kobes and H. Zaraket, Phys. Rev. D **58** (1998) 085003 [hep-ph/9804224].

- [17] F. D. Steffen and M. H. Thoma, Phys. Lett. B **510** (2001) 98 [hep-ph/0103044].
- [18] H. Nadeau, J. Kapusta and P. Lichard, Phys. Rev. C **45** (1992) 3034; **47** (1993) 2426.
- [19] L. Xiong, E. Shuryak and G. E. Brown, Phys. Rev. D **46**, 3798 (1992) [hep-ph/9208206].
- [20] P. Aurenche, Nucl. Phys. Proc. Suppl. **96** (2001) 179 [hep-ph/0009015].
- [21] C. T. Traxler, H. Vija and M. H. Thoma, Phys. Lett. B **346** (1995) 329 [hep-ph/9410309].
- [22] F. Karsch, Nucl. Phys. A **698** (2002) 199 [hep-ph/0103314].
- [23] F. Karsch, E. Laermann, P. Petreczky, S. Stickan and I. Wetzorke, hep-lat/0110208.
- [24] J. Sollfrank, P. Huovinen, M. Kataja, P. V. Ruuskanen, M. Prakash and R. Venugopalan, Phys. Rev. C **55** (1997) 392 [nucl-th/9607029].
- [25] P. F. Kolb, J. Sollfrank and U. Heinz, Phys. Rev. C **62** (2000) 054909 [hep-ph/0006129].
- [26] K. J. Eskola, K. Kajantie, P. V. Ruuskanen and K. Tuominen, Nucl. Phys. B **570** (2000) 379 [hep-ph/9909456].
- [27] C. Gale, Nucl. Phys. A **698** (2002) 143 [hep-ph/0104235].